



GOLD NANOCLOUDS SYNTHESIZED USING SOYBEAN TRYPSIN INHIBITOR (STI) WITH EXCELLENT BRIGHTNESS AND APPLICATION FOR THE DETECTION OF Hg²⁺

Helena T.N.N Amunyela, Yuliang Cheng, Yunfei Xie, Hang Yu, Weirong Yao, Yahui Guo* and He Qian

International Research Laboratory of Food Safety, Collaborative Innovation Centre of Food Safety and Quality Control in Jiangsu Province, Jiangnan University, Wuxi 214122, China

ARTICLE INFO

Article History:

Received 10th December, 2018

Received in revised form 2nd

January, 2019

Accepted 26th February, 2019

Published online 28th March, 2019

Key words:

Gold nanoclusters, soybean trypsin inhibitor, visual detection, mercury detection

ABSTRACT

Lately, the applications of metal nanomaterials are continuously increasing in numerous areas. However, during production, some of these methods can be hazardous to the environment, plants, and animals. Thus, there is a need for environmental friendly of metal nanomaterials during production. In this research, gold nanoclusters (Au NCs) were synthesized a new natural enzyme protein soybean trypsin inhibitor (STI) as protecting ligand. The results showed that the newly synthesized STI-Au NCs exhibited a very strong red fluorescence emission at 689 nm and excitation 513 nm. Optimum favourable conditions such as STI concentrations, buffers and time for the synthesis of STI-Au NCs were studied for the brightest fluorescence emission. This newly synthesized STI-Au NCs was used for the detection of mercury (Hg²⁺). The linear ship range for the Hg²⁺ ions is from 0.01 - 0.05 μ M with a detection limit of 0.71 nM. Additionally, this fluorescence STI-Au NCs probe can be easily synthesized and have generated a high fluorescence, hence, broadening its application in various fields of nanoscience.

Copyright©2019 **Helena T.N.N Amunyela et al.** This is an open access article distributed under the Creative Commons Attribution License, which permits unrestricted use, distribution, and reproduction in any medium, provided the original work is properly cited.

INTRODUCTION

Gold (Au) is well known as the noblest metal [1] and for the past thousands of years, gold has been widely used in society to make various items such as jewelry, coins, gold bars and decoration. This shiny, yellow, soft, precious and chemically inert metal recently became a hot area of research whereby tiny amounts of gold are being extensively studied to meet the urgent demands in many areas ranging from polluted water treatments, sensors for the detection of metal ions, small molecules, nucleic acids, proteins, bio-sensing, bio-imaging, bio-labelling, drug delivery, gene delivery, therapy, etc. in various fields of nanotechnology, biotechnology and biomedicine [2-5]. Different from gold colloid, commonly known as gold nanoparticles (Au NPs), gold nanoclusters (Au NCs) are on average approximately two nm or less in diameter and made up of a few to hundreds of gold atoms, a size that is comparable to the Fermi wavelength of electrons [6, 7]. The formation and properties of nanoclusters are assumed to be influenced by the amino acid contents and sequences in the protein template [8]. Fluorescent Au NCs have interesting unusual distinctive physiochemical properties, for example, ultra-small size, excellent solubility and stability in ambient conditions,

low toxicity, as well as good biocompatibility [9, 10]. Lately, the use of metal nanomaterials is rapidly increasing in numerous areas. However, during production some of these preparation methods can be harmful to our environment, plants, and animals, [11] therefore multiple of efforts have been committed to synthesizing high fluorescent Au NCs with better stability, improved brightness and of course environmentally friendly. [12] Among many of these approaches, protein protected Au NCs provided several outstanding distinct properties making it predominantly attractive. Protein protected Au NCs are friendly to the environment, require mild reaction conditions, exceptional water solubility, and biocompatibility [13]. The bovine serum albumin (BSA), [14, 15] egg white, [16] trypsin, [17, 18] pepsin, [19] lysozyme, [20, 21] insulin, [22, 23] human transferrin, [24, 25] and lactoferrin [26] are some of the commonly used proteins for the synthesis of Au NCs.

Soybean trypsin inhibitors (STI) also known as serine protease enzymes are responsible for decreasing the biological activity of trypsin and chymotrypsin enzymes, which can hinder the health of animals and humans when consumed [27, 28]. It was previously reported that majority of the legumes protein content on average ranges between 20% and 30% whereas for soybeans protein is much higher approximately at 40%, higher than other food sources such as meat, fish, cheese, egg, bread, rice, milk, etc. [29] STI is considered as a monomeric protein containing 181 amino acid residues in a single polypeptide chain cross-linked by two disulfide bridges with a molecular

***Corresponding author: Yahui Guo**

International Research Laboratory of Food Safety, Collaborative Innovation Centre of Food Safety and Quality Control in Jiangsu Province, Jiangnan University, Wuxi 214122, China

weight of 20.1 kDa. Soybean seed consist of Arginine (7.71 %), Alanine (4.02 %), Aspartic acid (6.88 %), Cysteine (2.50 %), Glutamic acid (19.01 %), Isoleucine (5.15 %), Leucine (8.16 %), Lysine (6.83 %), Phenylalanine (5.62 %), proline (5.29 %) and Serine (5.40 %) [30]. Xie's team in 2009, demonstrated that protein rich in amino acids residues (tyrosine and cysteine) play an important role in generating protein-protected Au NCs by acting as reducing and protective agents to reduce Au (III) to Au(0) [14]. Therefore making STI a potential ideal candidate.

Mercury (Hg) is a naturally occurring element that can be found in the air, soil, and water and is among one of the highly hazardous and well-known pollutants in the biological system with bio-accumulative properties [31]. Over-ingestion of mercury could lead to severe health effects to the central nervous system, endocrine systems, brain, liver, kidney and even death by interacting with thiol groups in protein and amino phospholipids [32]. Of late various testing approaches have been focused towards the detection of Hg^{2+} , for example, photo luminescent carbon nanomaterials, [33] atomic spectrometry, [34] inductively coupled plasma-mass spectrometry, [35] colorimetric sensors, [36] electrochemical analysis, [37] and surface-enhanced Raman spectroscopy [38]. Nonetheless, most of these methods are not user friendly, require expensive instruments and are not environmental friendly, unlike proteins. Consequently, this approach has the potentially be used for the detection of mercury for food safety, public health and environmental monitoring applications.

To the best of our knowledge, there has been no report on the use of STI as a template for the synthesis of Au NCs and application towards the detection of mercury (Hg^{2+}) ions. Herein, we report on the synthesis for Au NCs using the natural enzyme protein STI and the results obtained show a red strong fluorescence at a maximum excitation and emission wavelengths were 513 nm and 689 nm. The experiment was carried out at room temperature. Moreover, this newly synthesized STI-Au NCs was carried out successfully without requiring extra reducing and protecting agents and was further applied towards the detection of mercury (Hg^{2+}).

Experimental

Reagents and Materials

STI (Glycine max) was purchased from Sigma-Aldrich Trade Co., Ltd. (Shanghai, China). Hydrogen tetrachloroaurate ($H AuCl_4 \cdot 3H_2O$) was purchased Sinopharm Chemical Reagent Co., Ltd. (Shanghai, China). Tris-buffer, PBS, HEPES ($C_8H_{18}N_2O_4S$) and Sodium hydroxide (NaOH) were purchased from Sinopharm Chemical Reagent Co., Ltd. (Shanghai, China). Ultra-distilled water was collected from a Milli-Q A10 filtration system (Millipore, Billerica, MA, USA) and was used throughout the experiments. All the other chemicals were analytical grade.

Instrumentation

The fluorescence measurements were carried out on a spectro fluorophotometer RF-6000, Shimadzu Inc., (Kyoto, Japan) upon a maximum excitation of 513nm. Fluorescence images were performed on a transilluminator imaging system (Tanon 5200), Tianlong equipment factory (Shanghai, China) under UV light (302nm). Aqueous solutions were mixed thoroughly on a vortex mixer MX-F, Dragon Laboratory Instruments

Limited (Beijing, China). The transmission electron microscope (TEM) images were examined via a JEOL JEM-2100 HR (JEOL, Tokyo, Japan) at an accelerating voltage of 200 kV.

Synthesis of STI Au NCs

$H AuCl_4$ (0.01 M, 5 mL) was added to a 5 mL aqueous solution containing soybean trypsin inhibitor (STI) (30 mg/ mL), under mild stirring for 10 min to form a homogeneous solution on a vortex mixer. Sodium hydroxide (NaOH, 1 M) was added to adjust the solution mixture to a pH of 10. The mixed solution was then incubated at 37 °C for 20 h under mild stirring (120 rpm), according to previously reported approach [14]. The color of the reaction mixture changed from light yellow before incubation to deep brown after incubation.

Fluorescence Detection

Detection of STI-Au NCs fluorescence

After incubation, the STI-AuNCs (50 μ L) was added to tris-buffer (350 μ L, 0.01 M, pH 7) and mixed thoroughly prior to recording the fluorescence intensities. The experiment was carried out in independent triplicates.

Detection of Hg^{2+} fluorescence using STI-Au NCs

Different concentrations of Hg^{2+} in aqueous solution were freshly prepared using Tris-buffer (0.01 M, pH 7) and mixed thoroughly prior to use. The prepared solution was then mixed with STI-AuNCs (50 μ L) with a ratio of 7:1. The fluorescence spectra were recorded on a spectro fluorophotometer RF-6000, Shimadzu Inc., (Kyoto, Japan) at a maximum excitation of 513 nm. Applying the same conditions, different heavy metal ions were also examined individually in the presence of STI-Au NCs. The experiment was carried out in triplicates and the average fluorescence intensities were recorded as mentioned above.

RESULTS AND DISCUSSION

Synthesis and Characterization of STI-Au NCs

Several experiments were carried out to obtain the optimum favourable conditions for the synthesis of Au NCs producing a high fluorescence intensity. Important factors such as STI concentration, time and temperature for synthesizing were considered as clearly shown in Fig 1a, and Fig 1b. Four different concentrations (20 mg/ mL, 30 mg/ mL, 40 mg/ mL and 50 mg/ mL of Au NCs) were studied and the concentration of 40 mg/ mL produced the highest emission. However, the fluorescence emission produced by 30 mg/ mL did not show a significant difference in comparison to the other higher concentrations 40 mg/ mL and 50 mg/ mL, hence the 30 mg/ mL was used throughout the experiment. The lowest concentration of 20 mg/ mL resulted in Au NCs producing the lowest fluorescence intensity. The fluorescence intensity was recorded at different times with the interval of 2 h, and the highest fluorescence intensity was found to be at 20 h. The temperature was selected based on the previously reported results [14, 15], and 37 °C was favored due to its production of high fluorescence intensity.

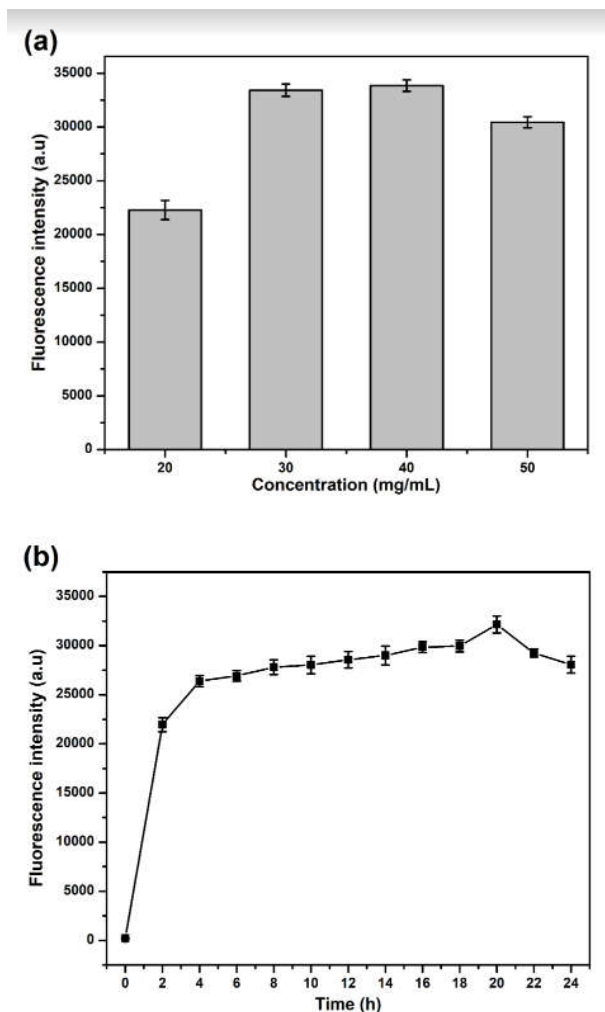


Fig 1(a) Fluorescence emission of four different concentrations (20 mg/ mL, 30 mg/ mL, 40 mg/ mL and 50 mg/ mL of STI-Au NCs. (b) Fluorescence emission spectra of 30 mg/ mL of STI-Au NCs under different times (0-24 h).

The morphology and particle size of the STI-Au NCs were studied using the TEM as shown in Fig 2a; the image displayed that the STI-Au NCs were uniformly well distributed, and almost spherical with an average diameter of less than 2.224 nm as shown in Fig 2a, inset. The newly synthesized STI-Au NCs maximum excitation and emission wavelengths were recorded at 513 nm and 689 nm, Fig 2b.

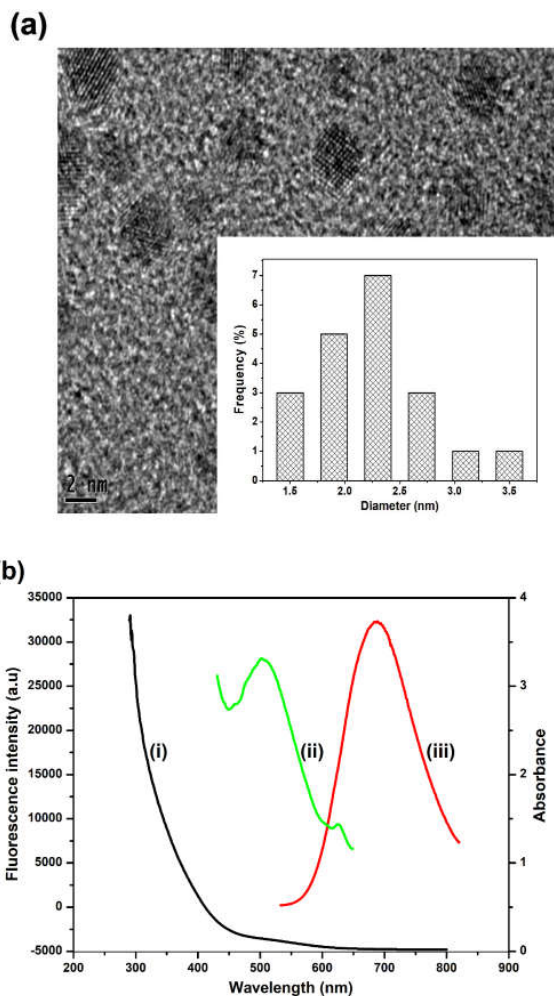


Fig 2 (a) TEM image of STI-Au NCs and the inset shows the size distribution of STI-Au NCs. (b) UV-visible absorption spectrum (i), excitation spectrum at 513 nm (ii) and fluorescence emission spectrum at 689 nm (iii).

Detection of Hg²⁺ using STI – Au NCs

The Mechanism for the Determination of Hg²⁺

Previous studies suggested that because of the Au⁺ (4f¹⁴5d¹⁰) and Hg²⁺ (4f¹⁴5d¹⁰) metallophilic interactions, Hg²⁺ is able to induce photoluminescence quenching of Au NCs [14, 39, 40]. Based on that, STI- Au NCs also stands a chance to be used as a fluorescence sensor towards the detection of Hg²⁺. As predicted, upon adding 0.05 μM Hg²⁺ to the STI-Au NCs solution, the fluorescence emission intensity significantly decreased, Fig 3. The red fluorescence of STI-Au NCs was quenched by 0.05 μM Hg²⁺, Fig 3, inset.

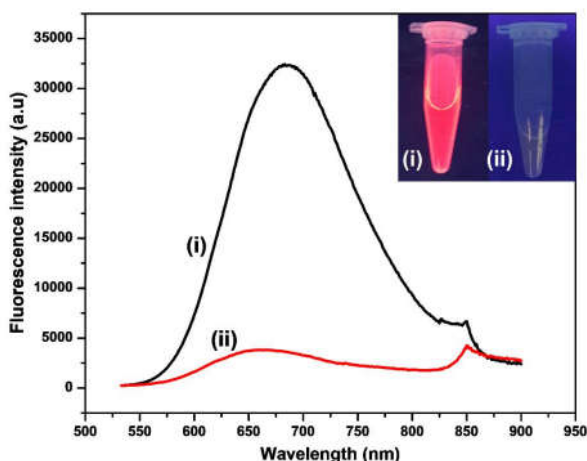


Fig 3 Fluorescence spectra of STI-Au NCs (i) in the absence and (ii) in the presence of 0.05 μM Hg^{2+} and inset images of STI-Au NCs (i) in the absence and (ii) in the presence of 0.05 μM Hg^{2+} under UV light at 302 nm.

Effects of Buffer on STI-Au NCs for the detection of Hg^{2+}

A series of tests were carried out to study the effects of three different buffers (Tris, PBS, and HEPES) (0.02 M, pH 7) on the fluorescence intensity of STI-Au NCs for Hg^{2+} (0.05 μM) detection. Fig 4, showed the images of the above-mentioned buffers under ultraviolet light at 302 nm. A decrease in the fluorescence emission was observed in Tris-buffer contrasting to HEPES and PBS. Thus, Tris-buffer was chosen as the suitable solvent for this approach to detect Hg^{2+} .

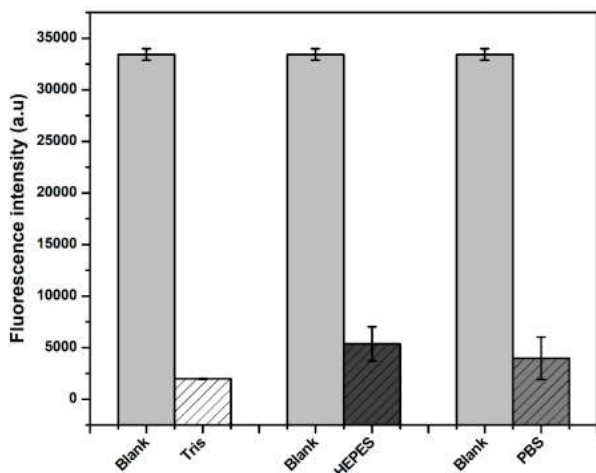


Fig 4 Comparison of three buffers (Tris-buffer, HEPES and PBS), each buffer had a concentration of Hg^{2+} at 0.05 μM .

Sensitivity of the STI-Au NCs for the Detection of Hg^{2+}

The sensitivity of STI-Au NCs was studied based on the optimal factors that were obtained. The fluorescence intensity of STI-Au NCs in the presence of different concentrations of Hg^{2+} ions (0, 0.01, 0.02, 0.03, 0.04, 0.05, 0.06, 0.07, 0.08, 0.09 and to 0.1 μM) were selected to examine the corresponding relation. It was observed that the fluorescence intensity of STI-Au NCs efficiently decreased with the increase in the concentration of Hg^{2+} , Fig 5a. The linear relationship between the fluorescence intensity and the concentration of Hg^{2+} correlated in the range 0.01 μM to 0.05 μM , respectively and the linear regression equation obtained was $y = -578242.45975x + 33318.54163$, $R^2 = 0.98933$ which indicated a good linear relationship, as shown in Fig 5a inset. Fig 5b illustrates the images of the STI-Au NCs in the presence of

different concentrations of Hg^{2+} ions from 0 μM to 0.1 μM under UV light (302 nm) irradiated under UV at 302 nm.

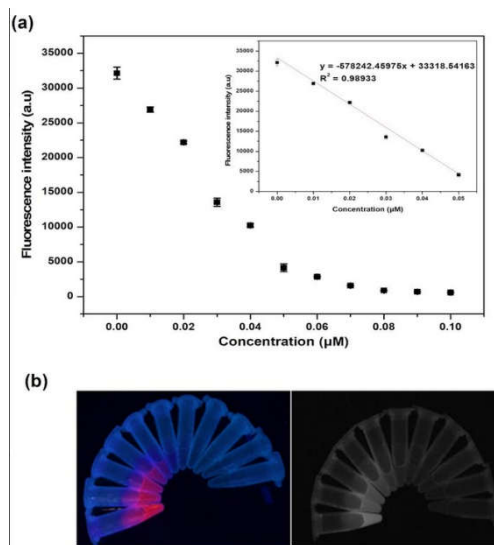


Fig 5 (a) Fluorescence emission intensities of STI-Au NCs in the presence of different concentrations of Hg^{2+} ions (0, 0.01, 0.02, 0.03, 0.04, 0.05, 0.06, 0.07, 0.08, 0.09 and to 0.1 μM). Inset shows the linear relationship between the fluorescence intensity and the concentration of Hg^{2+} from 0.01 μM to 0.05. (b) The images of STI-Au NCs in the presence of different concentrations of Hg^{2+} ions from 0 μM to 0.1 μM under UV light (302 nm) taken by phone camera and image system respectively.

Selectivity of the STI-Au NCs for the Detection of Hg^{2+}

Common heavy metal ions, such as Zn (II), Ca (II), Mg (II), Na (I), K (I), Pb (II), Fe (III), Co (II), Ni (II), and Cu (II) at 0.05 μM , were tested using the as-synthesized STI-Au NCs fluorescent for the selectivity of Hg^{2+} at a concentration of 10 mM. The results shown in Fig 6a, indicate that Hg^{2+} induces a visible fluorescence change at 689 nm. The Hg^{2+} quenched on to the fluorescence intensity of STI-Au NCs due to the high-affinity of metallophilic Hg^{2+} - Au^+ interactions, [41] whereas the other ions had little or no quenching effects on the fluorescence STI-Au NCs. Thus, making the newly synthesized STI-Au NCs a suitable sensor for selective & sensitive detection of Hg^{2+} . It was also observed that the red emission produced by the synthesized STI-Au NCs disappeared when it interacted with the Hg^{2+} , however, the other metal ions kept emitting the red fluorescence. Hence, the selectivity of Hg^{2+} could be easily visualized under UV light (302 nm), Fig 6b.

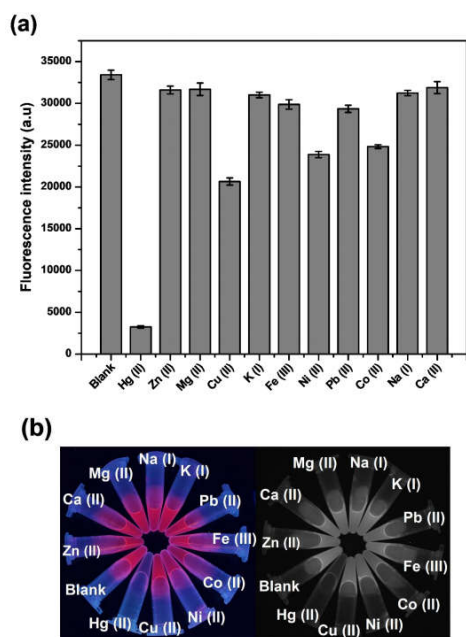


Fig 6 (a) Fluorescence emission intensities of different heavy metal ions at a concentration of 0.05 μM . (b) The UV-light pictures taken by phone camera (left) and image system (right) respectively. UV light at 302 nm.

Determination of Hg²⁺ in real Water Samples: Recovery – A case of Lake Water

The STI-Au NCs was further applied towards the detection of Hg²⁺ level in real water samples collected from Taihu Lake (Wuxi, Jiangsu, China) near Jiangnan University. The samples were then filtered through a 0.45 μm membrane for the removal of unwanted particles. The pre-treated water samples were mixed with Tris-buffer 0.01 M, pH 7 (1:1) and made different concentrations ranging from 0.01 μM to 0.06 μM of Hg²⁺. The above-prepared solutions were further mixed with STI-Au NCs solutions (50 μL), ratio 7:1 and the fluorescence spectra emission were recorded on a spectro fluorophotometer RF-6000, Shimadzu Inc., (Kyoto, Japan). The obtained Hg²⁺ recoveries ranged between 133 % and 106 % and an RSD below 8.2 % as shown in Table 1. The recovery percentage decreased to 100 % as the concentration of Hg²⁺ increases, thus making STI-Au NCs sensitive to the presence of Hg²⁺ ions.

Table 1 Determination of Hg²⁺ ions from Taihu-Lake water samples at 0.03, 0.04 and 0.05 μM concentrations.

Sample	Hg ²⁺ added (μM)	Hg ²⁺ detected (μM)	Recovery (%)	RSD % (n=3)
Lake water	0.03	0.040	133.30	8.21
	0.40	0.047	117.50	0.98
	0.05	0.053	106.00	3.45

RSD relative standard deviation

CONCLUSION

In summary, we successfully synthesized Au NCs using a natural enzyme protein soybean trypsin inhibitor (STI). This newly synthesized STI-Au NCs displayed a strong red fluorescence emission at 689 nm. The developed fluorescence probe was used to detect Hg²⁺ whereby the Hg²⁺ quenched the fluorescence of STI-Au NCs and could detect Hg²⁺ concentrations as little as 10 nM. This approach is less complicated (simple and straightforward), efficient, selective and sensitive towards the visual detection of Hg²⁺. Additionally, the newly developed fluorescence STI-Au NCs probe has the potential to be applied for biomaging, labelling,

sensing and therapy in numerous fields of nanoscience. Also, this approach could be further extended in the future to various types of protein protected metal NCs while maintaining good bioactivities.

Conflicts of interest

The authors declare no conflict of interest.

Acknowledgements

The work described in this article was supported by National Key Technology R & D Program in the 13th Five Year Plan of China (2018YFC160015, 2017YFC1601700), National first-class discipline program of Food Science and Technology (JUFSTR20180509), Science and technology project of Jiangsu Bureau of Quality and Technical Supervision (KJ175923 and KJ185646), and the “HongKong Scholar” programme.

References

1. Hammer, B. and J.K. Norskov, *Why gold is the noblest of all the metals*. Nature, 1995. 376(6537): p. 238-240.
2. Li, J., J.-J. Zhu, and K. Xu, *Fluorescent metal nanoclusters: From synthesis to applications*. Trends in Analytical Chemistry, 2014. 58: p. 90-98.
3. Zheng, Y., et al., *Recent advances in biomedical applications of fluorescent gold nanoclusters*. Advances in Colloid and Interface Science, 2017. 242: p. 1-16.
4. Zha, F., et al., *Tubular Micro/Nanomotors: Propulsion Mechanisms, Fabrication Techniques and Applications*. Micromachines (Basel), 2018. 9(2): p. 1-26.
5. Luo, M., et al., *Micro-/Nanorobots at Work in Active Drug Delivery*. Advanced Functional Materials, 2018. 28: p. 1706100.
6. de Heer, W.A., *The physics of simple metal clusters: experimental aspects and simple models*. Reviews of Modern Physics, 1993. 65(3): p. 611-676.
7. Chen, L.Y., et al., *Fluorescent gold nanoclusters: recent advances in sensing and imaging*. Analytical Chemistry, 2015. 87(1): p. 216-29.
8. Yaolin Xu, J.S., Ying Qin, b Dorothy Crowley, Marco Bonizzoni and Yuping Bao, *The role of protein characteristics in the formation and fluorescence of Au nanoclusters*. Nanoscale, 2014. 6(1515): p. 1515–1524.
9. Cui, M., Y. Zhao, and Q. Song, *Synthesis, optical properties and applications of ultra-small luminescent gold nanoclusters*. Trends in Analytical Chemistry, 2014. 57: p. 73-82.
10. Wei, H. and E. Wang, *Nanomaterials with enzyme-like characteristics (nanozymes): next-generation artificial enzymes*. Chemical Society Reviews, 2013. 42(14): p. 6060-93.
11. Joško, I., P. Oleszczuk, and E. Skwarek, *Toxicity of combined mixtures of nanoparticles to plants*. Journal of hazardous materials, 2017. 331: p. 200-209.
12. Qu, X., et al., *Fluorescent Gold Nanoclusters: Synthesis and Recent Biological Application*. Journal of Nanomaterials, 2015. 2015: p. 1-23.
13. Hu, Y., W. Guo, and H. Wei, *Protein- and Peptide-directed Approaches to Fluorescent Metal Nanoclusters*. Israel Journal of Chemistry, 2015. 55(6-7): p. 682-697.

14. Jianping Xie, Y.Z., and Jackie Y. Ying, *Protein-Directed Synthesis of Highly Fluorescent Gold Nanoclusters*. *Journal of Agricultural and Food Chemistry*, 2009. 131(3): p. 888-889.
15. Hu, L., et al., *Highly sensitive fluorescent detection of trypsin based on BSA-stabilized gold nanoclusters*. *Biosens Bioelectron*, 2012. 32(1): p. 297-9.
16. Dickson Josepha, K.E.G., *Synthesis of highly fluorescent gold nanoclusters using egg white proteins*. Elsevier - Colloids and Surfaces B: Biointerfaces 2014. 115: p. 46–50.
17. Yang, X., et al., *Novel synthesis of gold nanoclusters templated with L-tyrosine for selective analyzing tyrosinase*. *Analytica Chimica Acta*, 2014. 840: p. 87-92.
18. Jing-Min Liu, J.-T.C., and Xiu-Ping Yan, *Near Infrared Fluorescent Trypsin Stabilized Gold Nanoclusters as Surface Plasmon Enhanced Energy Transfer Biosensor and in Vivo Cancer Imaging Bioprobe*. *Analytical Chemistry*, 2013. 85: p. 3238–3245.
19. Kawasaki, H., et al., *ph-Dependent Synthesis of Pepsin-Mediated Gold Nanoclusters with Blue Green and Red Fluorescent Emission*. *Advanced Functional Materials*, 2011. 21(18): p. 3508-3515.
20. Liu, J., et al., *One-pot synthesis of gold nanoclusters with bright red fluorescence and good biorecognition abilities for visualization fluorescence enhancement detection of E. coli*. *Talanta*, 2015. 134: p. 54-9.
21. Wei, H., et al., *Lysozyme-stabilized gold fluorescent cluster: Synthesis and application as Hg(2+) sensor*. *Analyst*, 2010. 135(6): p. 1406-10.
22. Garcia, A.R., et al., *Human insulin fibril-assisted synthesis of fluorescent gold nanoclusters in alkaline media under physiological temperature*. *Colloids Surf B Biointerfaces*, 2013. 105: p. 167-72.
23. Liu, C.L., et al., *Insulin-directed synthesis of fluorescent gold nanoclusters: preservation of insulin bioactivity and versatility in cell imaging*. *Angewandte Chemie International Edition* 2011. 50(31): p. 7056-7060.
24. Le Guevel, X., N. Daum, and M. Schneider, *Synthesis and characterization of human transferrin-stabilized gold nanoclusters*. *Nanotechnology*, 2011. 22(27): p. 275103.
25. Choi, C.H., et al., *Mechanism of active targeting in solid tumors with transferrin-containing gold nanoparticles*. *Proceedings of the National Academy of Sciences*, 2010. 107(3): p. 1235-1240.
26. Xavier, P.L., et al., *Luminescent quantum clusters of gold in transferrin family protein, lactoferrin exhibiting FRET*. *Nanoscale*, 2010. 2(12): p. 2769-76.
27. Chanphai, P., L. Kreplak, and H.A. Tajmir-Riahi, *Aggregation of trypsin and trypsin inhibitor by Al cation*. *Journal of Photochemistry & Photobiology, B: Biology*, 2017. 169: p. 7-12.
28. Li, J., et al., *Inactivation of soybean trypsin inhibitor by dielectric-barrier discharge (DBD) plasma*. *Food Chemistry*, 2017. 232: p. 515-522.
29. Messina, M.J., *Legumes and soybeans: overview of their nutritional profiles and health effects*. *The American journal of clinical nutrition*, 1999. 70(3): p. 439s-450s.
30. Vagadia, B.H., S.K. Vanga, and V. Raghavan, *Inactivation methods of soybean trypsin inhibitor – A review*. *Trends in Food Science & Technology*, 2017. 64: p. 115-125.
31. Guedron, S., et al., *Mercury contamination level and speciation inventory in Lakes Titicaca & Uru-Uru (Bolivia): Current status and future trends*. *Environmental Pollution*, 2017. 231(Pt 1): p. 262-270.
32. Sun, Q., et al., *Postsynthetically Modified Covalent Organic Frameworks for Efficient and Effective Mercury Removal*. *Journal of the American Chemical Society*, 2017. 139(7): p. 2786-2793.
33. Hou, J., et al., *Nitrogen-doped photoluminescent carbon nanospheres: green, simple synthesis via hair and application as a sensor for Hg²⁺ ions*. *RSC Advances*, 2014. 4(70): p. 37342.
34. Hu, P., et al., *Speciation of mercury by hydride generation ultraviolet atomization-atomic fluorescence spectrometry without chromatographic separation*. *Microchemical Journal*, 2018. 143: p. 228-233.
35. Wohlmann, W., et al., *Development of an electrothermal vaporizer for direct mercury determination in soil by inductively-coupled plasma mass spectrometry*. *Spectrochimica Acta Part B: Atomic Spectroscopy*, 2018. 149: p. 222-228.
36. Hai, J., et al., *Porous Wood Members-Based Amplified Colorimetric Sensor for Hg(2+) Detection through Hg(2+)-Triggered Methylene Blue Reduction Reactions*. *Analytical Chemistry*, 2018. 90(7): p. 4909-4915.
37. Martín-Yerga, D. and A. Costa-García, *Recent advances in the electrochemical detection of mercury*. *Current Opinion in Electrochemistry*, 2017. 3(1): p. 91-96.
38. Wu, Y., et al., *Novel ratiometric surface-enhanced raman spectroscopy aptasensor for sensitive and reproducible sensing of Hg(2)*. *Biosens Bioelectron*, 2018. 99: p. 646-652.
39. Zhang, Y., et al., *Bright far-red/near-infrared gold nanoclusters for highly selective and ultra-sensitive detection of Hg²⁺*. *Sensors and Actuators B: Chemical*, 2017. 238: p. 683-692.
40. Li, H., et al., *The mechanism and application of the protein-stabilized gold nanocluster sensing system*. *Analyst*, 2017. 142(4): p. 567-581.
41. Sun, J. and Y. Jin, *Fluorescent Au nanoclusters: recent progress and sensing applications*. *Journal of Materials Chemistry C*, 2014. 2(38): p. 8000-8011.

How to cite this article:

Helena T.N.N Amunyela et al (2019) 'Gold Nanoclusters Synthesized Using Soybean Trypsin Inhibitor (Sti) with Excellent Brightness and Application for the Detection of Hg²⁺', *International Journal of Current Advanced Research*, 08(03), pp. 17750-17755. DOI: <http://dx.doi.org/10.24327/ijcar.2019.17755.3377>
